scientific reports

Check for updates

OPEN

Predicting outcomes of unruptured intracranial artery dissection with clear symptoms onset using clinical and radiological features

Yun Hwa Roh[1,2], Seung Chai Jung[1]✉, Minjae Kim[1], Hye Hyeon Moon[1], Pae Sun Suh[1,3], Yunsun Song[1], Ji Sung Lee[4] & Keum Mi Choi[1]

We investigated the clinical and radiologic predictors of unruptured symptomatic intracranial artery dissection (IAD) outcomes. Unruptured symptomatic IAD patients who underwent vessel wall magnetic resonance imaging (VW-MRI) and time-of-flight magnetic resonance angiography (TOF-MRA) within 1 month after symptom onset, followed for over 12 months were included. Baseline features predicting the clinical outcome of recurrent symptoms and radiologic outcomes of aneurysmal dilatation and occlusion were analyzed using logistic regression analysis. The Kaplan–Meier method calculated the median time to morphological stability. Patients with aneurysmal dilatation were categorized into progressive and non-progressive enlargement subgroups. Seventy-three IADs from 65 patients were included. All patients showed benign clinical course (mRS 0–1). No baseline features were predictive of recurrent symptoms. Aneurysmal dilatation was associated with increased outer diameter in baseline VW-MRI (OR, 23.15; 95% CI, 3.78–141.75, $P < 0.001$) and TOF-MRA (OR, 10.81; 95% CI, 2.16–53.99, $P = 0.004$). Occlusion was inversely associated with preserved patency in baseline VW-MRI (OR, 0.1; 95% CI, 0.01–0.74, $P = 0.024$) and TOF-MRA (OR, 0.14; 95% CI, 0.02–0.98; $P = 0.048$). The median time to morphological stability was 3.9 months (95% CI, 3.16–5.5). While baseline features did not significantly differ between aneurysmal dilatation subgroups, follow-up imaging revealed significant differences in remodeling index, normalized wall index, relative signal intensity of intramural hematoma, and presence of onion-skin appearance and intramural hematoma (all $P < 0.05$). Our findings suggest that while unruptured IAD presents a benign clinical outcome, follow-up imaging may be necessary to monitor the progressive enlargement of aneurysmal dilatation.

Keywords Dissection, Dissecting aneurysm, Vessel wall, Magnetic resonance imaging, Magnetic resonance angiography

Spontaneous intracranial artery dissection (IAD) is an uncommon but significant cause of stroke among younger and middle-aged patients[1]. The incidence of IAD is higher in Asian populations, predominantly affecting the posterior circulation and showing a predominance in men, whereas it is less common and more frequently involves the anterior circulation in Western populations[1,2]. IAD has varied morphology based on the pathogenesis and time that has passed since the IAD. Sub-intimal IAD tends to result in luminal steno-occlusion, while a sub-adventitial IAD tends to result in aneurysmal dilatation, also known as dissecting aneurysm[1,3,4]. Rapid morphological changes are a unique hallmark of IAD, occurring within 2–3 months and rarely after 6 months following symptom onset[3,5].

Unruptured IAD follows a typically benign course compared to ruptured IAD which has fatal clinical outcomes[6–10]. However, recurrent ischemic strokes may occur in 2–38% of IAD patients initially presenting with ischemic strokes[1,11]. Unruptured IAD may exhibit progressive enlargement of aneurysmal dilatation, associated with a high rupture rate of 7.7%[12] and symptomatic mass effect[6,10,13], prompting endovascular or surgical

[1]Department of Radiology and Research Institute of Radiology, University of Ulsan College of Medicine, Asan Medical Center, 86 Olympicro-43-gil, Songpa-gu, Seoul 05505, Republic of Korea. [2]Department of RadiologySamsung Medical Center, Sungkyunkwan University School of Medicine, Seoul, Republic of Korea. [3]Department of Radiology, Yonsei University College of Medicine, Seoul, Republic of Korea. [4]Department of Clinical Epidemiology and Biostatistics, University of Ulsan College of Medicine, Asan Medical Center, Seoul, Republic of Korea. ✉email: dynamics79@gmail.com

intervention during follow-up. Previous studies have suggested that symptomatic presentation, smoking, hyperlipidemia, young age, presence of intramural hematoma, and large diameter are potential predictors of progressive enlargement of IAD initially presented as aneurysmal dilatation. However, the duration from symptom onset to initial work-up was unclear or not reported in these studies[6,7,12,14,15]. Further, whether IAD resulted in recanalization or occlusion could affect the clinical outcome of unruptured IAD[8,16–18]. Although studies have reported that the relative signal intensity of intramural hematoma[18] and contrast enhancement[17] in vessel wall magnetic resonance imaging (VW-MRI) were associated with the recanalization of unruptured IAD, these studies are limited by their short-term follow-up of less than a year.

VW-MRI and time-of-flight magnetic resonance angiography (TOF MRA) are widely used for diagnosing and as follow-up imaging modalities for IAD, owing to their lack of radiation hazard and low invasiveness, while offering radiological performance comparable to that of computed tomography angiography (CTA) and digital subtraction angiography (DSA)[19–21].

Therefore, we aimed to investigate the clinical and radiologic features using baseline and follow-up VW-MRI and TOF-MRA to predict the outcomes of unruptured symptomatic IAD, with a clearly defined symptom onset time and follow-up period over 12 months. Specifically, the radiologic outcome was assessed as the final morphology of aneurysmal dilatation or occlusion, and the clinical outcome was defined as the presence of recurrent symptoms.

Results

Patients characteristics

From 2016 to 2020, a total of 374 patients underwent VW-MRI and TOF-MRA for evaluation of IAD (Fig. 1). Of these, 309 patients were excluded for the following reasons: unknown symptom onset ($n=91$), underwent VW-MRI after 1 month of symptom onset ($n=110$), absence of follow-up imaging for over 12 months ($n=92$), and underwent endovascular treatment within 1 month ($n=16$). A total of 73 dissections from 65 patients (mean age, 46.7 ± 10.08 years old; 27 females) were included.

The baseline characteristics of the study population are presented in Table 1. The mean interval between symptom onset and baseline imaging was 13.3 days ($n=73$; range, 1–30 days) and the mean interval from baseline to final follow-up period was 29.9 months ($n=73$; range, 12–80 months). Two patients underwent endovascular treatment involving the insertion of a flow diverter due to progressive enlargement of the aneurysmal dilatation at 20 months and 30 months, respectively, after symptom onset. Among the 65 patients, 45 patients (69.2%) initially presented with ischemic symptoms and 20 patients (30.8%) initially presented with headaches. Patients were treated with aspirin ($n=52$, 80%), clopidogrel ($n=36$, 55.4%), or statin ($n=47$, 72.3%). During the follow-up outpatient visits, thirteen patients (20%) complained of mild recurrent symptoms or neurologic deficit with modified Rankin Scale (mRS) 1 and subsequently underwent CT or MRI for evaluation. However, no newly developed lesions were found on the images.

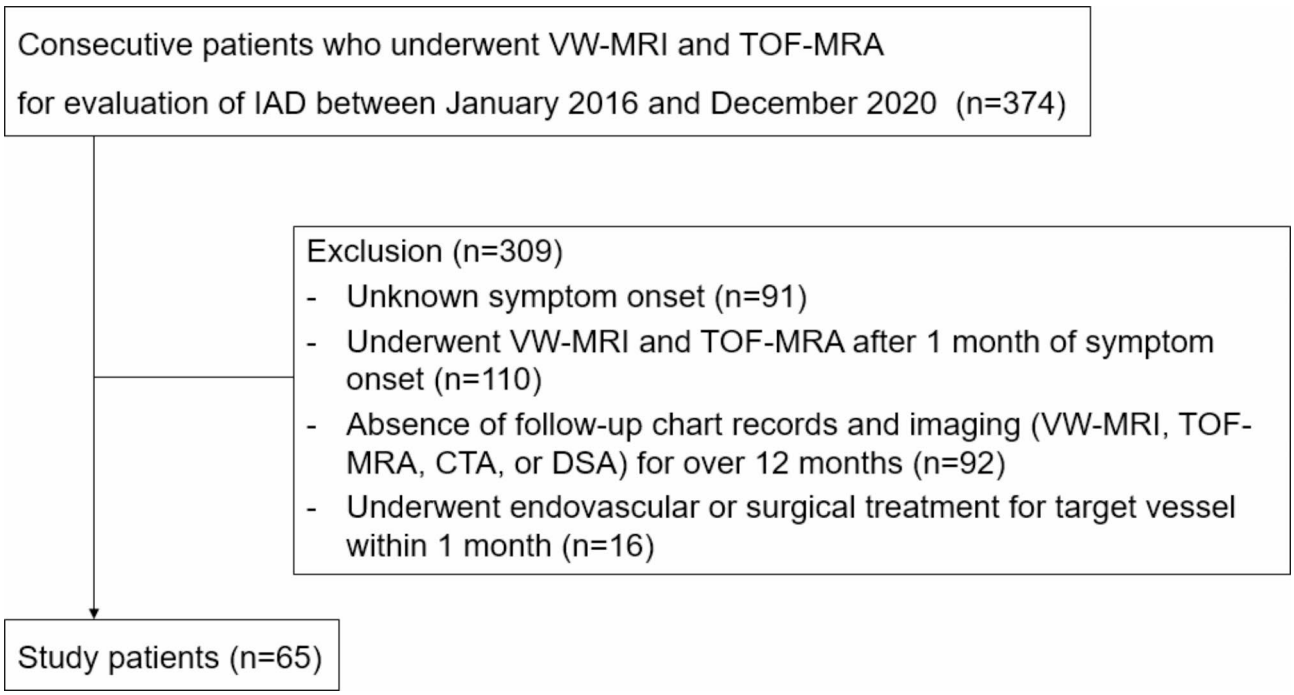

Fig. 1. Flowchart of participants. VW-MRI, vessel wall magnetic resonance image; IAD, intracranial artery dissection; TOF-MRA, time of flight-magnetic resonance angiography; CTA, computed tomography angiography; DSA, digital subtraction angiography.

	All patients ($n=65$)
Female	27 (41.5)
Age in years, mean ± standard deviation	46.8 ± 10.1
Hypertension	28 (43.1)
Diabetes	2 (3.1)
Hyperlipidemia	12 (18.5)
Smoking	21 (32.3)
Old cerebrovascular accident	3 (4.6)
Family history of stroke	13 (20)
Initial symptoms	
Ischemic symptom	45 (69.2)
Headache	20 (30.8)
Treatments	
Aspirin	52 (80)
Clopidogrel	36 (55.4)
Statin	47 (72.3)
Location of dissection ($n=73$)	
ACA	5 (6.8)
MCA	4 (5.5)
PCA	6 (8.2)
BA	2 (2.7)
VA	38 (52.1)
PICA	18 (24.7)
Clinical outcomes ($n=65$)	
Recurred or newly developed symptom	13 (20)
Headache	8 (12.3)
Dizziness	3 (4.6)
Ataxic gait	2 (3.1)
Asymptomatic	52 (80)
Final morphology ($n=73$)	
Aneurysmal dilatation	16 (21.9)
Progressive enlargement	7 (9.6)
Non-progressive enlargement	9 (12.3)
Occlusion	5 (6.8)
Incomplete normalization with residual stenosis	24 (32.9)
Complete normalization	28 (38.4)

Table 1. Baseline characteristics. Data are expressed as the number of cases with percentages in parentheses unless otherwise indicated. *ACA* anterior cerebral artery; *MCA* middle cerebral artery; *PCA* posterior cerebral artery; *BA* basilar artery; *VA* vertebral artery; *PICA* posterior inferior cerebellar artery.

Eight patients had dissections at more than one segment: four patients had dissections at the bilateral V4 segment of the vertebral artery (VA), one basilar artery (BA) and bilateral P4 segment of the posterior cerebral artery (PCA), and one at the BA and bilateral vertebral arteries. The most common location of dissection was the VA ($n=38$), followed by a posterior inferior cerebellar artery ($n=18$), PCA ($n=6$), anterior cerebral artery ($n=5$), middle cerebral artery ($n=4$), and BA ($n=2$). The final morphology was as follows: aneurysmal dilatation ($n=16$); occlusion ($n=5$); incomplete normalization with residual stenosis ($n=24$); complete normalization ($n=28$).

Comparisons of baseline features according to recurrent symptoms

There were no significant differences in the baseline clinical and radiologic features between the recurrence and non-recurrence symptom groups (Supplementary Table 2).

Comparisons of baseline features according to final morphology of aneurysmal dilatation and occlusion

The group with aneurysmal dilatation as the final morphology initially presented with headaches (75%), whereas those without aneurysmal dilatation mostly complained of ischemic symptoms (78.9%). The aneurysmal dilatation group showed a significantly higher proportion of increased outer diameter (93.8% vs. 12.3%, $P<0.001$) and larger remodeling index (3.224 vs. 2.058, $P=0.004$) and a less frequent presence of intramural hematoma (62.5% vs. 91.2%, $P=0.011$) at the baseline VW-MRI. Similarly, in the baseline TOF-MRA, the

	Aneurysmal dilatation ($n=16$)	No aneurysmal dilatation ($n=57$)	P	Occlusion ($n=5$)	No occlusion ($n=68$)	P
Male	8 (50)	33 (57.9)	0.574	3 (60)	38 (55.9)	1.000
Age in years, mean ± SD	49.5 ± 8.07	46.0 ± 10.5	0.224	49 ± 5.1	46.8 ± 10.1	0.613
Hypertension	6 (37.5)	24 (42.1)	0.741	3 (60)	27 (39.7)	0.396
Diabetes	1 (6.25)	1 (1.8)	0.393	0 (0)	2 (2.9)	1.000
Hyperlipidemia	2 (12.5)	11 (19.3)	0.720	0 (0)	13 (19.1)	0.578
Smoking	3 (18.9)	20 (35.1)	0.214	2 (40)	21 (30.9)	0.647
Old CVA	0 (0)	3 (5.3)	1.000	0 (0)	3 (4.4)	1.000
Family history	2 (12.5)	13 (22.8)	0.497	0 (0)	15 (22.1)	0.576
Initial symptom			< 0.001*			1.000
Ischemic symptom	4 (25)	45 (78.9)		3 (60)	46 (67.7)	
Headache	12 (75)	12 (21.1)		2 (40)	22 (32.4)	
Recurred or newly developed symptom	1 (6.3)	15 (26.3)	0.168	1 (20)	15 (22.1)	1.000
VW-MRI						
Dissecting flap	13 (81.3)	50 (87.7)	0.681	4 (80)	59 (86.8)	0.532
Double lumen	9 (56.3)	20 (35.1)	0.126	0 (0)	29 (42.7)	0.150
Intramural hematoma	10 (62.5)	52 (91.2)	0.011*	5 (100)	57 (83.8)	1.000
Increased outer diameter	15 (93.8)	7 (12.3)	< 0.001*	0 (0)	22 (32.4)	0.314
Onion-skin appearance	5 (31.3)	17 (29.8)	1.000	3 (60)	19 (27.9)	0.157
Wall enhancement	13 (81.3)	31 (54.4)	0.052	2 (40)	42 (61.8)	0.380
Preserved patency	15 (93.8)	38 (66.7)	0.054	1 (20)	52 (76.5)	0.018*
Eccentricity index[a]	0.49 (-0.07–0.86)	0.75 (0.49–0.86)	0.118	0.6 (0.5–0.72)	0.74 (0.43–0.86)	0.454
Remodeling index[a]	3.2 (2.44–4.22)	2.06 (1.6–3)	0.004*	2.53 (2.4–4.64)	2.33 (1.64–3.23)	0.303
Normalized wall index[a]	0.66 (0.53–0.77)	0.57 (0.5–0.69)	0.212	0.66 (0.56–0.69)	0.57 (0.51–0.7)	0.786
rsIMH[a]	1.63 (1.35–2.35)	2 (1.48–3.53)	0.086	3.13 (2.21–3.89)	1.87 (1.43–3.21)	0.247
TOF-MRA						
Dissecting flap	12 (75)	35 (61.4)	0.316	3 (60)	44 (64.7)	1.000
Double lumen	5 (31.3)	9 (15.8)	0.278	0 (0)	14 (20.6)	0.576
Intramural hematoma	7 (43.8)	26 (45.6)	0.895	4 (80)	29 (42.7)	0.169
Increased outer diameter	13 (81.3)	9 (15.8)	< 0.001*	0 (0)	22 (32.4)	0.314
Preserved patency	14 (87.5)	35 (61.4)	0.050	1 (20)	48 (70.6)	0.037
Remodeling index[a]	2.87 (2.02–4.35)	1.97 (1.19–2.77)	0.005*	2.45 (2.06–2.65)	2.1 (1.28–3.33)	0.860
rsIMH[a]	2.2 (1.27–2.64)	1.56 (1.13–2.53)	0.142	2.53 (1.86–2.85)	1.62 (1.16–2.59)	0.110

Table 2. Comparison of baseline features according to final morphology. Data are expressed as the number of cases with percentages in parentheses unless otherwise indicated. [a]Data are expressed as median (interquartile range). *VW-MR* vessel wall magnetic resonance image; *TOF-MRA* time of flight-magnetic resonance angiography; *SD* standard deviation; *CVA* cerebrovascular accident; *rsIMH* relative signal intensity of intramural hematoma. * indicates statistical significance ($P<0.05$).

aneurysmal dilatation group also frequently demonstrated increased outer diameter (81.3% vs. 15.8%, $P<0.001$) and a larger remodeling index (2.866 vs. 1.973, $P=0.005$) (Table 2).

There were no significant differences in the baseline clinical characteristics between those with final morphology of occlusion and those without occlusion. The group without occlusion exhibited preserved patency in both baseline VW-MRI (76.5% vs. 20%, $P=0.018$) and TOF-MRA (70.6% vs. 20%, $P=0.037$) compared to the occlusion group.

Predicting recurrent symptom from baseline clinical and radiological features

No baseline clinical or radiological features could predict the recurrence of symptoms (Supplementary Table 3).

Predicting final morphology of aneurysmal dilatation and occlusion from baseline clinical and radiological features

In the multivariable logistic regression analysis, only increased diameter in both VW-MRI (odds ratio [OR], 26.08; 95% confidence interval [CI], 3.96–171.89; $P<0.001$) and TOF-MRA (OR, 11.53; 95% CI, 2.18–60.84, $P=0.004$) remained significantly associated with the outcome of aneurysmal dilatation (Table 3).

The final morphology of occlusion was inversely associated with the baseline feature of preserved patency in both VW-MRI (OR, 0.1; 95% CI, 0.01–0.74, $P=0.024$) and TOF-MRA (OR, 0.14; 95% CI, 0.02–0.98; $P=0.048$) (Table 4).

	Univariate		Multivariable (1)		Multivariable (2)	
	OR (95% CI)	P	OR (95% CI)	P	OR (95% CI)	P
Male	0.73 (0.24–2.2)	0.577				
Age (per 10 years increase)	1.41 (0.78–2.54)	0.256				
Hypertension	0.85 (0.27–2.61)	0.771				
Diabetes	3.64 (0.22–61.68)	0.370				
Hyperlipidemia	0.70 (0.15–3.25)	0.646				
Smoking	0.47 (0.13–1.77)	0.267				
Old CVA	0.47 (0.01–15.11)	0.671				
Family history	0.57 (0.12–2.59)	0.465				
Initial symptom						
Ischemic symptom	1(Ref)		1(Ref)		1(Ref)	
Headache	10.11 (2.86–35.78)	< 0.001*	2.45 (0.37–16.08)	0.35	2.89 (0.50–16.79)	0.237
VW-MRI						
Dissecting flap	0.57 (0.13–2.47)	0.455				
Double lumen	2.32 (0.76–7.06)	0.139				
Intramural hematoma	0.17 (0.04–0.66)	0.011*	0.40 (0.04–4.02)	0.437	0.27 (0.04–1.88)	0.187
Increased outer diameter	69.58 (10.76–449.83)	< 0.001*	26.08 (3.96–171.89)	< 0.001*		
Onion-like appearance	1.11 (0.34–3.61)	0.867				
Wall enhancement	3.25 (0.88–11.96)	0.077				
Preserved patency	5.23 (0.86–31.75)	0.072				
Eccentricity index (per 0.1 unit increase)	0.88 (0.78–0.99)	0.036*				
Remodeling index	1.38 (1.02–1.87)	0.034*				
Normalized wall index (per 0.1 unit increase)	1.33 (0.87–2.05)	0.190				
RsIMH	0.63 (0.35–1.13)	0.120				
TOF-MRA						
Dissecting flap	1.76 (0.52–5.96)	0.363				
Double lumen	2.44 (0.69–8.66)	0.167				
Intramural hematoma	0.94 (0.31–2.83)	0.910				
Increased outer diameter	19.69 (4.93–78.71)	< 0.001*			11.53 (2.18–60.84)	0.004*
Preserved patency	3.68 (0.85–15.99)	0.082				
Remodeling index	1.54 (1.08–2.19)	0.017*	1.34 (0.67–2.68)	0.408	1.42 (0.77–2.62)	0.261
rsIMH	1.46 (0.80–2.67)	0.217				

Table 3. Logistic regression analysis on baseline features predicting aneurysmal dilatation. *VW-MRI* vessel wall magnetic resonance image; *TOF-MRA* time of flight-magnetic resonance angiography; *OR* odds ratio; *CI* confidential interval; CVA, cerebrovascular accident; *rsIMH*,relative signal intensity of intramural hematoma. Multivariable analysis was performed with two separate models to address the issue of multicollinearity involving the variable 'increased outer diameter.' In the first model, the variable of increased outer diameter on TOF-MRA was excluded. In the second model, the variable of increased outer diameter on VW-MRI was excluded. * indicates statistical significance ($P < 0.05$).

Analysis of progressive enlargement of aneurysmal dilatation and morphological stability

Within the aneurysmal dilatation group of 16 IAD lesions, seven were categorized as the progressive enlargement group and nine as the non-progressive aneurysmal dilatation group. There were no significant differences in the baseline clinical and radiological features between the two groups (Supplementary Table 4).

In the IAD lesions that exhibited no further morphological changes, the median time from symptom onset to morphological stability was 3.9 months (95% CI, 3.16–5.5 months) (Fig. 2). Based on these findings, further analyses were conducted on the groups with progressive and non-progressive enlargement of aneurysmal dilatation using the mid-term follow-up imaging performed later than 4 months after the symptom onset. When the groups were compared using imaging taken at a similar time, all four cases in the progressive enlargement group displayed an onion-skin appearance in VW-MRI and intramural hematoma in TOF-MRA. They also demonstrated a larger remodeling index in both VW-MRI (16.56 vs. 2.39, $P = 0.021$) and TOF-MRA (12.96 vs. 2.01, $P = 0.021$), and an increased normalized wall index (0.975 vs. 0.67, $P = 0.021$) and rsIMH (4.6 vs. 1.38, $P = 0.021$) in VW-MRI (Table 5). Representative cases are displayed in Fig. 3.

	OR (95% CI)	*P*
Male	1.11 (0.20–6.16)	0.906
Age (per 10 years increase)	1.21 (0.50–2.92)	0.671
Hypertension	2.11 (0.38–11.76)	0.393
Diabetes	2.42 (0.05–110.33)	0.650
Hyperlipidemia	0.37 (0.02–7.97)	0.528
Smoking	1.58 (0.28–8.90)	0.605
Old CVA	1.70 (0.05–58.17)	0.768
Family history	0.31 (0.02–6.56)	0.455
Initial symptom		
Ischemic symptom	1(Ref)	
Headache	1.48 (0.26–8.30)	0.658
VW-MRI		
Dissecting flap	0.48 (0.06–3.71)	0.481
Double lumen	0.12 (0.01–2.40)	0.166
Intramural hematoma	2.20 (0.10–48.12)	0.617
Increased outer diameter	0.19 (0.01–3.78)	0.275
Onion-skin appearance	3.55 (0.63–20.08)	0.151
Wall enhancement	0.45 (0.08–2.48)	0.356
Preserved patency	0.10 (0.01–0.74)	0.024*
Eccentricity index (per 0.1 unit increase)	0.97 (0.81–1.17)	0.769
Remodeling index	1.27 (0.87–1.84)	0.211
Normalized wall index (per 0.1 unit increase)	0.74 (0.44–1.26)	0.271
rsIMH	1.66 (0.81–3.41)	0.167
TOF-MRA		
Dissecting flap	0.77 (0.14–4.32)	0.767
Double lumen	0.34 (0.02–7.21)	0.490
Intramural hematoma	4.02 (0.58–27.77)	0.159
Increased outer diameter	0.19 (0.01–3.78)	0.275
Preserved patency	0.14 (0.02–0.98)	0.048*
Remodeling index	1.06 (0.64–1.75)	0.833
rsIMH	1.73 (0.72–4.13)	0.218

Table 4. Logistic regression analysis on baseline features predicting occlusion. *VW-MRI* vessel wall magnetic resonance image; *TOF-MRA* time of flight-magnetic resonance angiography; *OR* odds ratio; *CI* confidential interval; *CVA* cerebrovascular accident; *rsIMH* relative signal intensity of intramural hematoma. * indicates statistical significance ($P < 0.05$).

Discussion

None of the baseline clinical or radiological features were predictive of recurrent symptoms. The baseline radiological features of increased outer diameter and lack of luminal patency in both VW-MRI and TOF-MRA were significant predictors of aneurysmal dilatation and occlusion as the final morphology, respectively ($P < 0.05$). The median time from symptoms onset to morphological stability was 3.9 months. The baseline clinical and radiological features were not significantly different between the groups with progressive and non-progressive enlargement of aneurysmal dilatation. However, the progressive enlargement group exhibited a significantly larger remodeling index in both VW-MRI and TOF-MRA, a higher rate of onion-skin appearance, a larger normalized wall index, and rsIMH in VW-MRI ($P < 0.05$) at the mid-term follow-up. The progressive enlargement group also showed a more frequent presence of intramural hematoma in TOF-MRA ($P < 0.05$).

The clinical outcomes of unruptured symptomatic IAD are generally benign, with the recurrence rates of ischemic stroke reported to range between 2–14%[1,6–10], and more than 80% of patients maintained a mRS < 2[22–24]. In our study, none of the patients experienced hemorrhage or recurrent stroke during the follow-up period, and those who complained of recurrent symptoms or neurologic deficits (13/65, 20%) exhibited only a mild form as estimated with mRS 1.

The major morphological changes in IAD usually occur within 2–3 months after symptom onset, and these changes generally end within 6–7 months[4,11,25]. It is rare for such changes to occur for more than 6 months after the onset of symptoms[3,5]. Our study findings align with the previous findings demonstrating that the median time interval for observing morphological stability in IAD was approximately 4 months following symptoms onset.

The progressive enlargement of aneurysmal dilatation in unruptured IAD during follow-ups is critical to establish the need for an endovascular or surgical intervention. Although one of the most common radiological features predicting progressive enlargement of IAD was baseline large diameter, many of these studies did not

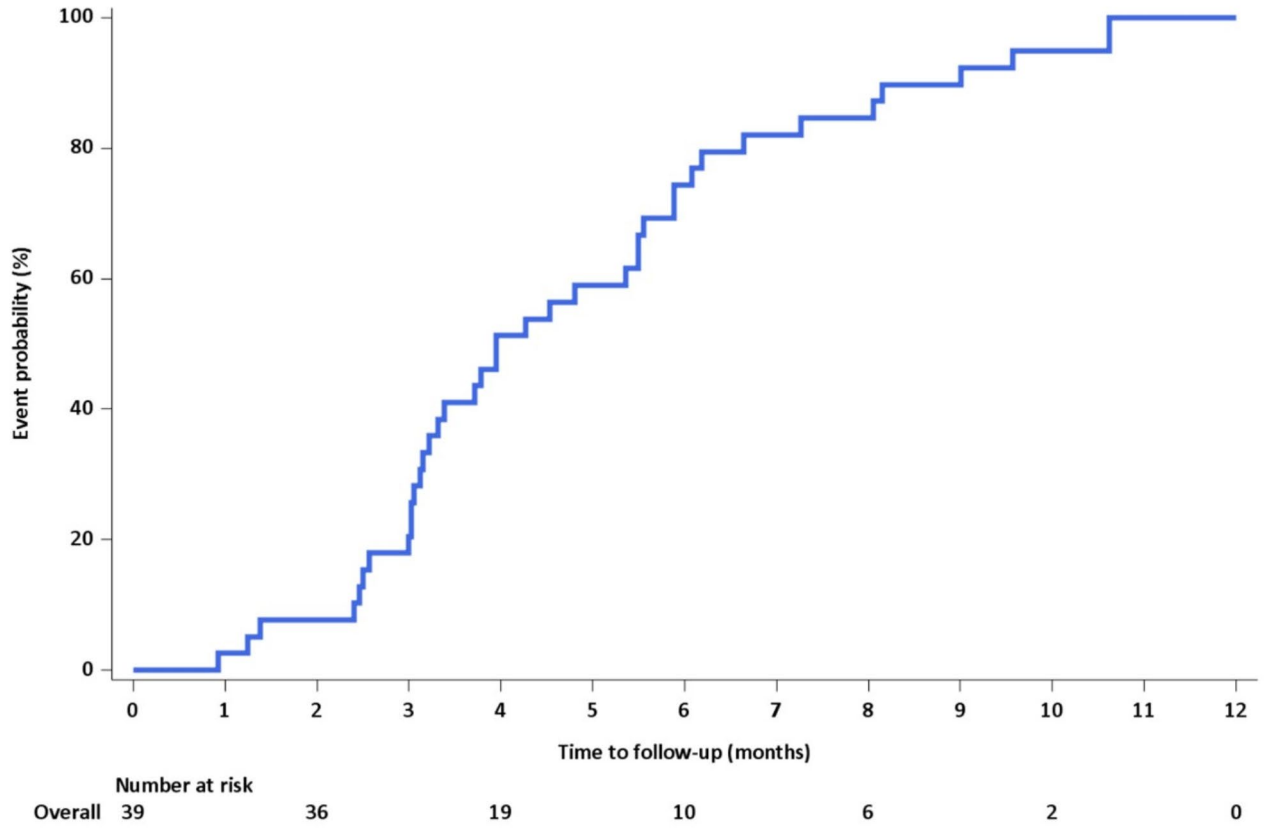

Fig. 2. Time from symptom onset to angiographic stabilization. The Kaplan–Meier curve illustrates time from the onset of symptoms to the point of angiographic stabilization, as evidenced by no further changes in the shape of the intracranial artery dissection when compared to the last follow-up image. The median time from symptom onset to morphological stability is 3.9 months (95% confidence interval, 3.16–5.5 months).

clearly report the time interval between the onset of symptoms and the initial imaging[6,7,10,12,14,15]. However, this information is significant because IAD can exhibit clinical and radiological changes within days or even hours after symptom onset[3,4,11,22]. Further, if the exact onset time is unknown, the baseline features of IAD initially identified on imaging may not be the initial features since the onset of symptoms but instead be indicative of features that occur after the acute to subacute stage (the most vigorous phase of morphological change). In our study, the baseline feature of increased outer diameter was the only predictor of the final morphology of aneurysmal dilatation. There were no significant differences in the baseline features between the progressive and non-progressive enlargement of aneurysmal dilatation groups within 1 month. However, follow-up imaging conducted after 4 months showed distinguishable features between the two groups. Therefore, collectively, findings from the previous studies and our present study results, an initial imaging alone may not fully capture the dynamic process of IAD.

In our study, the group with aneurysmal dilatation as the final morphology initially presented with headaches, whereas those without aneurysmal dilatation predominantly complained of ischemic symptoms. Patients with aneurysmal dilatation mostly showed preserved patency, which likely explains their lesser association with ischemic symptoms. Similar findings have been reported in previous research on intracranial unruptured vertebrobasilar artery dissection, showing that non-ischemic patients more frequently exhibited aneurysmal dilatation while ischemic patients more often showed steno-occlusive lesions[24]. Another study also reported that vertebrobasilar artery dissection patients who presented with isolated headaches had a higher rate of arterial dilatation and more dynamic arterial changes during follow-up[26]. Headaches in IAD may result from a direct tear of the blood vessel wall, where mechanical tears of the arterial wall usually extend to the sub-adventitial layer[27], potentially associated with aneurysmal enlargement.

Recanalization and luminal patency are also important features to predict clinical outcomes in unruptured IAD[8,16–18], although a study by Wadhwa et al. reported that the likelihood of good neurological outcome was not influenced by the recanalization status[9]. Hashimoto et al. reported that after a mean follow-up interval of 52 days, a higher contrast enhancement in unruptured IAD was associated with increasing stenosis or aneurysmal dilatation[17]. They also reported that after 3 months of follow-up imaging, higher rsIMH was associated with recanalization or the attenuation of the vascular morphology[18]. However, these studies did not show specific results on recanalization or luminal patency, and were limited by short-term follow-ups. Lin et al. demonstrated that the presence of a double lumen and occlusion were associated with no remodeling in cervico-cranial

	Progressive enlargement of aneurysmal dilatation ($n=4$)	Non-progressive aneurysmal dilatation ($n=4$)	*P*
Time to MRI from symptom onset, days	216 (196–231)	182.0 (157–193.5)	0.083
Male	3 (75)	2 (50)	1.000
Age, years	48.5 (46–53.5)	42.5 (39–50.5)	0.245
Initial symptom			0.429
Ischemic symptom	2 (50)	0 (0)	
Headache	2 (50)	4 (100)	
Hypertension	2 (50)	0 (0)	0.429
Diabetes	1 (25)	0 (0)	1.000
Hyperlipidemia	1 (25)	1 (25)	1.000
Smoking	1 (25)	2 (50)	1.000
Old CVA	0 (0)	0 (0)	
Family history	0 (0)	1 (25)	1.000
VW-MRI			
Dissecting flap	4 (100)	2 (50)	0.429
Double lumen	4 (100)	1 (25)	0.143
Intramural hematoma	4 (100)	1 (25)	0.143
Increased outer diameter	4 (100)	4 (100)	NA
Onion-skin appearance	4 (100)	0 (0)	0.029*
Wall enhancement	4 (100)	2 (50)	0.429
Preserved patency	4 (100)	3 (75)	1.000
Eccentricity index	0.84 (0.74–0.94)	0.54 (0.39–0.72)	0.059
Remodeling index	16.56 (7.80–24.71)	2.39 (2.11–2.97)	0.021*
Normalized wall index	0.98 (0.96–0.99)	0.67 (0.65–0.76)	0.021*
rsIMH	4.60 (3.21–4.92)	1.38 (1.24–1.46)	0.021*
TOF-MRA			
Dissecting flap	4 (100)	2 (50)	0.429
Double lumen	4 (100)	1 (25)	0.143
Intramural hematoma	4 (100)	0 (0)	0.029*
Increased outer diameter	3 (75)	3 (75)	1.000
Preserved patency	3 (75)	3 (75)	1.000
Remodeling index	12.96 (7.47–19.2)	2.02 (1.66–2.89)	0.021*
rsIMH	2.67 (1.91–3.28)	1.07 (0.96–2.16)	0.149

Table 5. Comparisons of follow-up features between progressive enlargement and non-progressive aneurysmal dilatation. Data are expressed as the number of cases with percentages in parentheses or median (interquartile range). *VW-MRI* vessel wall magnetic resonance image; *TOF-MRA* time of flight-magnetic resonance angiography; *CVA* cerebrovascular accident; *rsIMH* relative signal intensity of intramural hematoma. * indicates statistical significance ($P<0.05$).

artery dissection, but their study included extracranial artery dissections and medial follow-up interval was 8.5 months[28]. Our study addresses this gap by demonstrating that the status of luminal patency in baseline imaging can be a predictor of occlusion as the final morphology, after a minimum follow-up period of 12 months. Similarly, Nedeltchev et al. demonstrated that occlusion at 1-month ultrasonography reduced the likelihood of recanalization at 12 month follow-up[29], but that study was limited to extracranial carotid artery dissection. To our knowledge, this is the first study to focus on the recanalization of IAD as extensively.

This study had several limitations. First, this was a retrospective study at a single center and involved a small number of patients. However, we included only unruptured symptomatic patients of IAD with clear time intervals from the symptom onset. Second, the imaging follow-up for each patient was irregular because of the retrospective study design. Third, the final morphology was classified on various angiography. Fourth, the lack of significant differences in baseline features between groups with progressive and non-progressive enlargement of aneurysmal dilatation could be attributed to the small number of study patients. Studies using a larger patient cohort are needed to validate the findings of our study. Finally, our study focused on symptomatic IAD with a clear symptom onset, and thus did not include asymptomatic IAD, which may exhibit fluctuating radiological findings during follow-up. Future research should consider including asymptomatic cases to provide a more comprehensive understanding of IAD.

In conclusion, unruptured symptomatic IAD demonstrated a benign clinical outcome. The baseline radiological features of increased outer diameter and lack of luminal patency were associated with aneurysmal dilatation and occlusion as the final morphology, respectively. A follow-up imaging may be necessary to monitor the progressive enlargement of aneurysmal dilatation.

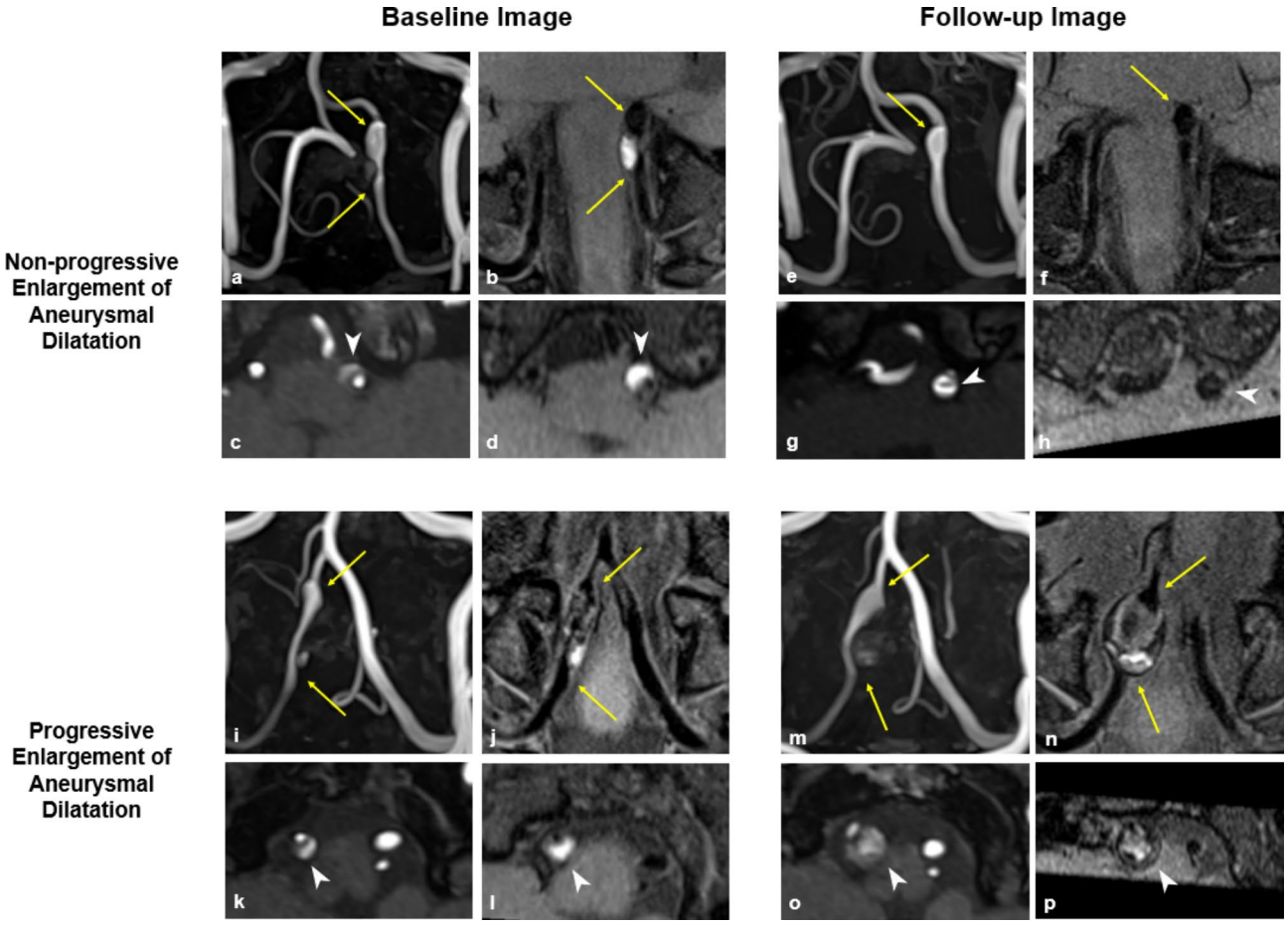

Fig. 3. Baseline and Follow-up Images in Cases of Non-progressive and Progressive Enlargement of Aneurysmal Dilatation. (**a–h**) Representative case of non-progressive enlargement of aneurysmal dilatation. (**a**, **b**) Baseline images show dissection in the left vertebral artery (arrow) with an increased outer diameter compared to the adjacent normal-looking artery. (**c**, **d**) Axial images at the point of maximal outer diameter shows double lumen with dissecting flap and intramural hematoma (arrow head). The remodeling index, normalized wall index, and relative signal intensity of intramural hematoma (rsIMH) were 2.49, 0.59, and 3.09, respectively. (**e**, **f**) Follow-up images after 6 months of symptom onset shows residual aneurysmal dilatation of the dissected artery (arrow). (**g**, **h**) Axial images demonstrates dissecting flap (arrow head) but no intramural hematoma in both TOF-MRA and VW-MRI. The remodeling index, normalized wall index, and rsIMH were 2.22, 0.64, and 1.33, respectively. (**i–p**) Representative case of progressive enlargement of aneurysmal dilatation. (**i**, **j**) Baseline images show dissection in the right vertebral artery (arrow) with an increased outer diameter. (**k**, **l**) Baseline axial images show double lumen with dissecting flap and intramural hematoma (arrow head). The remodeling index, normalized wall index, and rsIMH were 3.43, 0.67, and 3.94, respectively. (**m**, **n**) Follow-up images after 6 months of symptom onset show continuous enlargement in the diameter of the dissected artery (arrow). (**o**, **p**) Axial images demonstrate the onion-skin appearance of a multilayered hematoma. The remodeling index, normalized wall index, and rsIMH were 26.08, 0.99, and 4.89, respectively.

Methods

Study population

This retrospective observational cohort study was approved by the institutional review board at Asan Medical Center, and the requirement for informed consent was waived (IRB No. 2023 – 0294, date of approval: March 2023). All methods were performed in accordance with the principles outlined in the Declaration of Helsinki.

Consecutive patients who underwent VW-MRI and TOF-MRA for evaluation of IAD at our institution between January 2016 and December 2020 were reviewed. The inclusion criteria were as follows: (a) age ≥ 18 years, (b) IAD diagnosed based on clinical history and imaging (VW-MRI and TOF-MRA with or without CTA or DSA), (c) IAD which was not ruptured, traumatic, or iatrogenic. The exclusion criteria were as follows: (a) unclear symptoms onset, (b) did not undergo baseline VW-MRI and TOF-MRA within 1 month of symptom onset, (c) did not have follow-up chart records and imaging (VW-MRI, TOF-MRA, CTA, or DSA) for more than 12 months, (d) underwent endovascular treatment for target vessels.

Image acquisition

The VW-MRI was conducted using a 3.0-T MRI system (Magnetom Skyra; Siemens) with 64-channel head and neck coils using sampling perfection with application-optimized contrasts and different flip-angle evolutions (SPACE) and 3D turbo spin-echo sequences. The proton density images, T2-weighted images, pre-contrast T1-weighted images (T1WIs), and contrast-enhanced T1WIs were obtained using SPACE. The contrast-enhanced T1WIs were obtained after intravenous administration of gadoterate meglumine (Dotarem) at 0.1 mmol per kilogram of body weight. Additionally, 3D TOF-MRA was performed, and the imaging parameters are summarized in Supplementary Table 1.

Diagnosis of IAD

The diagnosis of IAD was based on definite signs of a dissecting flap and double lumen, along with suspicious signs of intramural hematoma, aneurysmal dilatation, and rapid morphological changes observed on follow-up imaging[1].

Imaging analysis

Two neuroradiologists (S.C.J. with 15 years of experience and Y.H.R. with 6 years of experience) analyzed VW-MRI and TOF-MRA images with consensus reading. The neurologists conducted the image analysis based on information on a picture archiving and communication system workstation (PetaVision®; Asan Medical Center) and AquariusNET viewer version 4.4.13 (TeraRecon, Durham), and were blinded to the clinical and laboratory characteristics of the patients.

The presence or absence of the following imaging characteristics measured using VW-MRI and TOF-MRA were analyzed at baseline in all patients, and at mid-term follow-up (5–8 months) in the group with aneurysmal dilatation: (1) dissecting flap, (2) double lumen, (3) intramural hematoma, (4) increased outer diameter (relative to the adjacent normal-appearing arteries), (5) preserved patency of the lumen. The onion-skin appearance and wall enhancement were assessed using VW-MRI only. The onion-skin appearance was defined as a multilayered thrombus or wall hematoma[30]. The wall enhancement was present if the enhancement degree was equal to or greater than the pituitary stalk[31].

The remodeling index and relative signal intensity of intramural hematoma (rsIMH) were assessed in VW-MRI and TOF-MRA. The remodeling index was calculated as the maximal outer wall area in the lesion site/mean value of the outer wall area in adjacent proximal and distal normal-looking arteries[32]. The rsIMH was calculated as the signal intensity in intramural hematoma/signal intensity in the masseter muscle on T1WI on VW-MRI and TOF-MRA[33]. In the case of absence of intramural hematoma, the rsIMH was calculated as the signal intensity of the vessel wall at the dissected artery/signal intensity in the masseter muscle. The normalized wall index and eccentricity index were assessed in VW-MRI. The normalized wall index was calculated as the wall area/maximal outer wall area[34]. The eccentricity index was calculated as (maximum wall thickness-opposite wall thickness)/maximum wall thickness.

Radiologic outcome: final morphology assessment

The final morphology was categorized into aneurysmal dilatation, occlusion, incomplete normalization, and complete normalization, based on findings from CTA, MRA, or DSA at the last follow-up imaging. Within the aneurysmal dilatation category, patients who exhibited continuous enlargement in diameter during follow-up were classified as the "progressive enlargement of aneurysmal dilatation", and those for whom the lesions did not show a progressive enlargement (i.e., no change or decreased size over time) were classified as "non-progressive aneurysmal dilatation." Incomplete normalization was defined as lesions showing residual stenosis while preserving patency, whereas complete normalization was defined when lesions appeared normal.

Each follow-up image was assessed to identify changes in angiographic shape relative to the previous image. The date at which changes in angiographic shape were not observed in comparison to the last follow-up image, was recorded and defined as the date of stability.

For the detection of recurrent infarcts from the baseline to the final follow-up, computed tomography, diffusion-weighted imaging, and fluid-attenuated inversion recovery were reviewed.

Clinical outcome

Two neuroradiologists (S.C.J. and Y.H.R.) conducted a consensus review of the patients' initial symptoms using the chart records. Initial symptoms were classified as either ischemic symptoms or headaches. During follow-up visits, chart records were thoroughly reviewed to document any symptoms the patient complained of. If the reported symptoms were severe enough to necessitate further imaging evaluation, they were recorded as recurrent symptoms.

Statistical analysis

The Chi-square test, Fisher's exact test, Student's *t*-test, and Wilcoxon rank sum test were used for comparisons of baseline clinical and radiological features according to recurrent symptoms (recurrence group and non-recurrence group) and final morphology (aneurysmal dilatation and occlusion). A multivariable logistic regression using Firth's penalized maximum likelihood method following a series of univariate analyses was used to identify independent features associated with recurrent symptoms, final morphology of aneurysmal dilatation or occlusion. Multivariable analysis was performed with two separate models to address the issue of multicollinearity involving the variable 'increased outer diameter' on VW-MRI and TOF-MRA.

The clinical and radiological features between non-progressive and progressive enlargement of aneurysmal dilatation were compared using Fisher's exact test and Mann– Whitney U test at baseline and mid-term follow-up imaging. The median time from the symptom onset to the date at which the angiographic shape demonstrated no further changes compared to the last follow-up image was calculated using the Kaplan– Meier method.

All statistical analyses were performed using IBM SPSS for Windows, Version 21.0 (Armonk, NY: IBM Corp) and MedCalc version 20.014 (MedCalc Software Ltd, Ostend, Belgium). All tests were two-sided, and a p-value < 0.05 was considered statistically significant.

Data availability

The data in the current study are available from the corresponding author upon reasonable request.

Received: 8 July 2024; Accepted: 17 September 2024
Published online: 01 October 2024

References

1. Debette, S. *et al.* Epidemiology, pathophysiology, diagnosis, and management of intracranial artery dissection. *Lancet Neurol.***14**, 640–654. https://doi.org/10.1016/S1474-4422(15)00009-5 (2015).
2. Ekker, M. S. *et al.* Epidemiology, aetiology, and management of ischaemic stroke in young adults. *Lancet Neurol.***17**, 790–801. https://doi.org/10.1016/S1474-4422(18)30233-3 (2018).
3. Schievink, W. I. Spontaneous dissection of the carotid and vertebral arteries. *N. Engl. J. Med.***344**, 898–906. https://doi.org/10.1056/NEJM200103223441206 (2001).
4. Mizutani, T. Natural course of intracranial arterial dissections. *J. Neurosurg.***114**, 1037–1044. https://doi.org/10.3171/2010.9.JNS10668 (2011).
5. Lee, S. H., Kim, K. Y. & Jung, J. M. High-resolution magnetic resonance imaging for the follow-up of intracranial arterial dissections. *Acta Neurol. Belg.***121**, 1599–1605. https://doi.org/10.1007/s13760-020-01432-0 (2021).
6. Kobayashi, N. *et al.* Natural course of dissecting vertebrobasilar artery aneurysms without stroke. *AJNR Am. J. Neuroradiol.***35**, 1371–1375. https://doi.org/10.3174/ajnr.A3873 (2014).
7. Sacho, R. H. *et al.* Natural history and outcome after treatment of unruptured intradural fusiform aneurysms. *Stroke***45**, 3251–3256. https://doi.org/10.1161/Strokeaha.114.006292 (2014).
8. Kuwabara, M. *et al.* Natural history of acute unruptured vertebral basilar artery dissection: Temporal changes in imaging findings and contributory factors. *Clin. Neurol. Neurosurg.*https://doi.org/10.1016/j.clineuro.2022.107450 (2022).
9. Wadhwa, A., Almekhlafi, M., Menon, B. K., Demchuk, A. M. & Bal, S. Recanalization and functional outcome in patients with cervico-cephalic arterial dissections. *Can. J. Neurol. Sci.***50**, 393–398. https://doi.org/10.1017/cjn.2022.40 (2023).
10. Moon, J. *et al.* Growth of asymptomatic intracranial fusiform aneurysms: Incidence and risk factors. *Clin. Neuroradiol.***29**, 717–723. https://doi.org/10.1007/s00062-018-0695-z (2019).
11. Bond, K. M., Krings, T., Lanzino, G. & Brinjikji, W. Intracranial dissections: A pictorial review of pathophysiology, imaging features, and natural history. *J. Neuroradiol.***48**, 176–188. https://doi.org/10.1016/j.neurad.2020.03.007 (2021).
12. Dmytriw, A. A., Alrashed, A., Enriquez-Marulanda, A., Medhi, G. & Pereira, V. M. Unruptured intradural posterior circulation dissecting/fusiform aneurysms natural history and treatment outcome. *Interv. Neuroradiol.***29**, 56–62. https://doi.org/10.1177/15910199211068673 (2023).
13. Sikkema, T. *et al.* Clinical features and prognosis of intracranial artery dissection. *Neurosurgery***76**, 663–670. https://doi.org/10.1227/NEU.0000000000000696 (2015).
14. Daou, B. *et al.* Dissecting pseudoaneurysms: Predictors of symptom occurrence, enlargement, clinical outcome, and treatment. *J. Neurosurg.***125**, 936–942. https://doi.org/10.3171/2015.10.Jns151846 (2016).
15. Horio, Y. *et al.* Factors predictive of enlargement of dissecting aneurysms in the vertebral artery. *World Neurosurg.***151**, E935–E942. https://doi.org/10.1016/j.wneu.2021.05.024 (2021).
16. Ahn, S. S. *et al.* Spontaneous symptomatic intracranial vertebrobasilar dissection: Initial and follow-up imaging findings. *Radiology***264**, 196–202. https://doi.org/10.1148/radiol.12112331 (2012).
17. Hashimoto, Y. *et al.* Magnetic resonance vessel wall imaging predicts morphological deterioration in unruptured intracranial artery dissection. *J. Stroke Cerebrovasc.*https://doi.org/10.1016/j.jstrokecerebrovasdis.2020.105006 (2020).
18. Hashimoto, Y. *et al.* Diagnostic accuracy of MR vessel wall imaging at 2 weeks to predict morphological healing of vertebral artery dissection. *J. Stroke Cerebrovasc.*https://doi.org/10.1016/j.jstrokecerebrovasdis.2022.106728 (2022).
19. Kaufmann, T. J. *et al.* Complications of diagnostic cerebral angiography: evaluation of 19,826 consecutive patients. *Radiology***243**, 812–819. https://doi.org/10.1148/radiol.2433060536 (2007).
20. Levy, C. *et al.* Carotid and vertebral artery dissections: three-dimensional time-of-flight MR angiography and MR imaging versus conventional angiography. *Radiology***190**, 97–103. https://doi.org/10.1148/radiology.190.1.8259436 (1994).
21. Mandell, D. M. *et al.* Intracranial Vessel Wall MRI: Principles and expert consensus recommendations of the american society of neuroradiology. *AJNR Am. J. Neuroradiol.***38**, 218–229. https://doi.org/10.3174/ajnr.A4893 (2017).
22. Ono, H. *et al.* Symptomatic recurrence of intracranial arterial dissections follow-up study of 143 consecutive cases and pathological investigation. *Stroke***44**, 126-U227. https://doi.org/10.1161/Strokeaha.112.670745 (2013).
23. Yamaura, A., Ono, J. & Hirai, S. Clinical picture of intracranial non-traumatic dissecting aneurysm. *Neuropathology***20**, 85–90. https://doi.org/10.1046/j.1440-1789.2000.00276.x (2000).
24. Kim, B. M. *et al.* Outcomes and prognostic factors of intracranial unruptured vertebrobasilar artery dissection. *Neurology***76**, 1735–1741. https://doi.org/10.1212/WNL.0b013e31821a7d94 (2011).
25. Jeon, Y. S., Cho, J., Park, J. J., Roh, H. G. & Chun, Y. I. Acute hemicranial pain accompanied with a pearl and string type dissection of intracranial vertebral artery: Consideration for the time when to finish the medical observation. *Medicine*. https://doi.org/10.1097/Md.0000000000032008 (2022).
26. Lee, S. J. *et al.* Significance of headache in intracranial vertebrobasilar artery dissections: An observational study. *Sci. Rep.***13**, 21653. https://doi.org/10.1038/s41598-023-48941-5 (2023).
27. Mehdi, E. *et al.* Craniocervical dissections: Radiologic findings, pitfalls, mimicking diseases: A pictorial review. *Curr. Med. Imaging Rev.***14**, 207–222. https://doi.org/10.2174/1573405613666170403102235 (2018).
28. Lin, X. *et al.* Initial and follow-up high-resolution vessel wall MRI study of spontaneous cervicocranial artery dissection. *Eur. Radiol.***34**, 1704–1715. https://doi.org/10.1007/s00330-023-10207-z (2024).
29. Nedeltchev, K. *et al.* R2-recanalization of spontaneous carotid artery dissection. *Stroke***40**, 499–504. https://doi.org/10.1161/STROKEAHA.108.519694 (2009).
30. Krings, T. & Choi, I. S. The many faces of intracranial arterial dissections. *Interv. Neuroradiol.***16**, 151–160. https://doi.org/10.1177/159101991001600206 (2010).

31. Qiao, Y. *et al.* Intracranial plaque enhancement in patients with cerebrovascular events on high-spatial-resolution MR images. *Radiology***271**, 534–542. https://doi.org/10.1148/radiol.13122812 (2014).
32. Zhu, X. J. *et al.* Morphologic characteristics of atherosclerotic middle cerebral arteries on 3T high-resolution MRI. *Am. J. Neuroradiol.***34**, 1717–1722. https://doi.org/10.3174/ajnr.A3573 (2013).
33. Hashimoto, Y. *et al.* Monitoring intramural hematoma on vessel wall imaging to evaluate the healing of intracranial vertebral artery dissection. *J. Stroke Cerebrovasc.*https://doi.org/10.1016/j.jstrokecerebrovasdis.2021.105992 (2021).
34. Qiao, Y. *et al.* MR imaging measures of intracranial atherosclerosis in a population-based study. *Radiology***280**, 860–868. https://doi.org/10.1148/radiol.2016151124 (2016).

Author contributions
Project administration and supervision: S.C.J., Data curation: S.C.J., Y.H.R., K.M.C., M.K., H.H.M., P.S.S., Y.S., Formal analysis: J.S.L., Methodology: S.C.J., Y.H.R., Writing—original draft: Y.H.R., Writing—review & editing: Y.H.R., S.C.J. All authors read and approved the final manuscript.

Funding
This study was supported by the National Research Foundation of Korea (NRF) grant funded by the Korean government (NRF-2020M3E5D2A01084578 and NRF-2019R1A2C1089939).

Declarations

Competing interests
The authors declare no competing interests.

Additional information
Supplementary Information The online version contains supplementary material available at https://doi.org/10.1038/s41598-024-73418-4.

Correspondence and requests for materials should be addressed to S.C.J.